Available online at www.sciencedirect.com
ScienceDirect
International Journal of Heat and Mass Transfer 50 (2007) 1435–1441
International Journal of HEAT and MASS TRANSFER
www.elsevier.com/locate/ijhmt

Numerical investigation of thermo-bioconvection in a suspension of gravitactic microorganisms

Z. Alloui, T.H. Nguyen, E. Bilgen *

Ecole Polytechnique, University of Montreal, C.P. 6079, Centre-ville, Montréal, Que. Canada H3C 3A7

Received 1 June 2006; received in revised form 8 September 2006
Available online 13 November 2006

Abstract

This paper investigates the effect of heating or cooling from below on the development of gravitactic bioconvection in a square enclosure with stress free sidewalls. The governing equations are the Navier–Stokes equations with the Boussinesq approximation, the diffusion equation for the motile microorganism and the energy equation for the temperature. The control volume method is used to solve numerically the complete set of governing equations. It was found that the suspension is destabilized by heating from below and stabilized by cooling from below. A transition from a subcritical bifurcation to a supercritical bifurcation was observed in the case of heating from below when the thermal Rayleigh number was increased.

Keywords: Bioconvection; Gravitactic microorganisms; Heated layer

1. Introduction

Bioconvection is the spontaneous pattern formation in suspensions of microorganisms which are little denser than water and move randomly, but on the average, upwardly against gravity. Up swimming of microorganisms is generally a response to an external force field such as gravity or biochemical stimulus such as gradient of oxygen concentration. Due to up swimming, the top layer of the suspension becomes denser than the layer below, resulting in an unstable density distribution. This may lead to a convective instability and formation of convection patterns similar to the patterns observed in Bénard convection. Theoretical models of bioconvection for different types of motile microorganisms have been developed in various recent publications [1–3]. For a review of the fundamental work in this area, see Pedley and Kessler [4] and Hill and Pedley [5].

Rational continuum models for a suspension of purely gravitactic microorganisms have been formulated and analysed by Childress et al. [6]. The formulation includes the Navier–Stokes equations with the Boussinesq approximation for an incompressible fluid and the microorganism conservation equation. A numerical study based on the equations derived by Childress et al. [6] was presented by Fujita and Watanabe [7]. They discretized the equations using finite differences method with a spatially staggered grid. They found that the system of bioconvection can lead into chaotic behavior via a sequence of bifurcations by increasing the Rayleigh number. The preferred wavenumber of gravitactic bioconvection in a rectangular cavity was studied by Harashima et al. [8] who carried out numerical experiments to show that the system evolves in the direction of intensifying downward advection of microorganisms and reducing the total potential energy of the system.

Ghorai and Hill [9–12] studied gyrotactic bioconvection in a series of papers using a vorticity–stream function formulation of the basic model first introduced by Pedley et al. [13]. They examined the development and instabilities of two-dimensional gyrotactic plumes. Cases with different initial conditions and different width-to-height ratios of a deep enclosure were compared.

* Corresponding author. Tel.: +1 514 340 4711x4579; fax: +1 514 340 5917.
E-mail address: bilgen@polymtl.ca (E. Bilgen).

0017-9310/$ - see front matter © 2006 Elsevier Ltd. All rights reserved.
doi:10.1016/j.ijheatmasstransfer.2006.09.008

Nomenclature

A	cavity aspect ratio, $A = L/H$
D_c	cell diffusivity
$\vec{g}$	gravitational acceleration
H	cavity height
$\vec{J}$	dimensionless flux of microorganisms
$\vec{k}$	unit vertical vector
L	cavity width
Le	Lewis number, $Le = \alpha/D_c$
n	dimensionless cell concentration
$\bar{n}$	average cell concentration
$\vec{n}$	unit normal vector to the boundaries
p	dimensionless pressure
Pe	bioconvection Peclet number, $Pe = HV_c/D_c$
Ra	bioconvection Rayleigh number, $Ra = g\vartheta\Delta\rho\bar{n}H^3/\rho\nu D_c$
Ra_T	thermal Rayleigh number, $Ra_T = g\beta\Delta T H^3/\nu\alpha$
Sc	Schmidt number, $Sc = \nu/D_c$
T	dimensionless temperature
t	dimensionless time
$\vec{u}$	dimensionless fluid velocity
V_c	gravitactic cell velocity
(x,y)	dimensionless coordinate system

Greek symbols

α	thermal diffusivity
β	volume expansion coefficient
ω	dimensionless vorticity
μ	dynamic viscosity of the suspension
ν	kinematic viscosity of the suspension
ρ_w	water density
ρ_c	cell density
$\Delta\rho$	difference between cell and water densities, $\Delta\rho = \rho_c - \rho_w$
ϑ	cell volume
ψ	dimensionless stream function

Superscripts

$'$	dimensional variable
sub	subcritical
sup	supercritical

Recently, a number of theoretical analyses of thermo-bioconvection of a suspension of gyrotactic and oxytactic microorganisms have been carried out by Kuznetsov [14–16]. Kuznetsov [14] investigated the effect of the temperature gradient on the stability of a suspension of motile gyrotactic microorganisms in a fluid layer. It is suggested that this problem may be relevant to motile thermophilic microorganisms that live in hot springs. The author found that a suspension of gyrotactic microorganisms in a horizontal fluid layer heated from below is less stable than the same suspension under isothermal conditions.

Nield and Kuznetsov [17] studied the case where the layer is cooled from below. They present a linear stability analysis of a suspension of gyrotactic microorganisms in fluid layer of finite depth. They found that cooling from below stabilizes the suspension and oscillatory convection is possible in certain circumstances. The present authors carried out a linear stability analysis of the thermo-bioconvection in suspension of gravitactic microorganisms in shallow fluid layers [18]. The effect of heating or cooling below on the stability was investigated. They found that the thermal effect may stabilize or destabilize the suspension and change the wave length of the bioconvection pattern.

We see from this brief review that there are as yet no numerical simulations of thermo-bioconvection flows above the critical Rayleigh numbers, all studies considered only the analytical solutions of the stability problem. This paper is concerned with the numerical investigation of the development of thermo-bioconvection in a rectangular enclosure with stress free sidewalls. Our interest will be focused on the effect of heating or cooling from below on the bifurcation diagrams of the suspension.

2. Mathematical formulation

The system consists of a suspension of gravitactic microorganisms enclosed in a two-dimensional rectangular cavity of width L and height H referred to Cartesian coordinates (x', y') with the y' axis pointing vertically upwards. The left and right walls of the cavity are stress-free and the top and bottom walls are rigid. There is no flux of cells through any of the walls. The computational domain and the thermal boundary conditions are shown in Fig. 1.

The equations solved are the two-dimensional Navier–Stokes equations with Boussinesq approximations, cell conservation equation and energy equation:

$$\nabla \cdot \vec{u}' = 0 \tag{1}$$

$$\rho_w \frac{\partial \vec{u}'}{\partial t'} + \rho_w \nabla \cdot (\vec{u}'\vec{u}') = -\nabla p' + \mu \nabla^2 \vec{u}' + \vartheta \Delta\rho n' \vec{g} - \rho_w \beta (T' - T_0)\vec{g} \tag{2}$$

$$\frac{\partial n'}{\partial t'} = -\nabla \vec{J}' \quad \text{with} \quad \vec{J}' = (\vec{u}' + V_c \vec{k}) n' - D_c \nabla n' \tag{3}$$

$$\frac{\partial T'}{\partial t'} + \nabla \cdot (\vec{u}' T') = \alpha \nabla^2 T' \tag{4}$$

The equations are scaled using the height H as the length-scale, D_c/H as the velocity scale, $\bar{n}$ as the concentration scale and ΔT as the temperature scale. By using the vorticity stream function formulation, we deduce the dimensionless system of coupled equations:

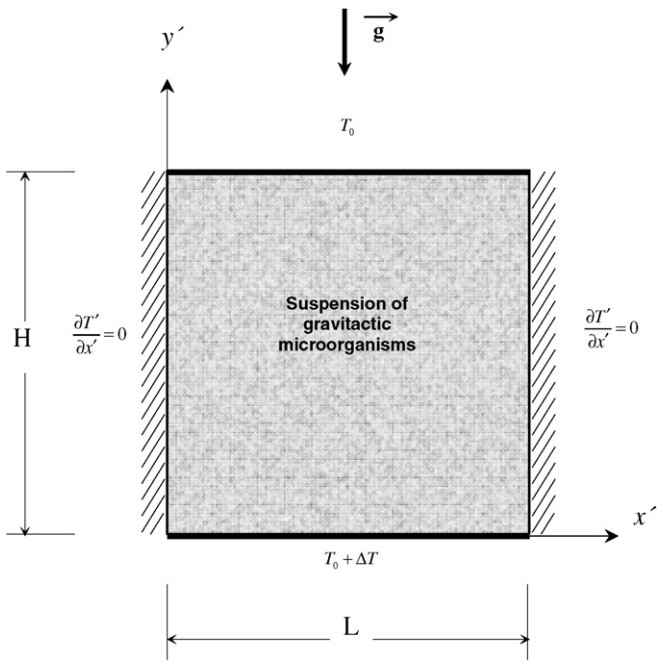

Fig. 1. Computational domain and thermal boundary conditions.

$$\omega = -\nabla^2\psi \tag{5}$$

$$\frac{\partial\omega}{\partial t} + u\frac{\partial\omega}{\partial x} + v\frac{\partial\omega}{\partial y} = Sc\nabla^2\omega + Sc\left(Ra\frac{\partial n}{\partial x} - Ra_T Le\frac{\partial T}{\partial x}\right) \tag{6}$$

$$\frac{\partial n}{\partial t} + u\frac{\partial n}{\partial x} + (v+Pe)\frac{\partial n}{\partial y} = \nabla^2 n \tag{7}$$

$$\frac{\partial T}{\partial t} + u\frac{\partial T}{\partial x} + v\frac{\partial T}{\partial y} = Le\nabla^2 T \tag{8}$$

where $Sc = \nu/D_c$, the Schmidt number, $Ra = g\vartheta\Delta\rho\bar{n}PeH^3/\rho\nu D_c$, the bioconvection Rayleigh number, $Ra_T = g\beta\Delta TH^3/\nu\alpha$, the thermal Rayleigh number, $Le = \alpha/D_c$, the Lewis number, and $Pe = HV_c/D_c$, the bioconvection Peclet number are the governing parameters of the problem.

We impose rigid, no-slip boundary conditions at the bottom and top walls and assume that the other boundaries are stress-free, so that

$$\psi = 0, \quad \frac{\partial\psi}{\partial y} = 0 \quad \text{at } y = 0, 1 \tag{9}$$

$$\psi = 0, \quad \frac{\partial^2\psi}{\partial x^2} = 0 \quad \text{at } x = 0, A \tag{10}$$

At the impermeable boundaries, the condition of zero-flux, are applied, i.e.,

$$\vec{J}\cdot\vec{n} = 0 \quad \text{at } x = 0, A \text{ and } y = 0, 1 \tag{11}$$

while the thermal boundary conditions are

$$T = 1 \quad \text{at } y = 0 \tag{12}$$

$$T = 0 \quad \text{at } y = 1 \tag{13}$$

$$\frac{\partial T}{\partial x} = 0 \quad \text{at } x = 0,\ A \tag{14}$$

The initial condition is given as follows

$$n = \bar{n}, \quad T = 0 \quad \text{at } t = 0 \tag{15}$$

3. Numerical procedure

The control volume method [19] is used to discretize the governing equations (5)–(8) with a uniform staggered grid. The stream function is stored on one set of nodes and the vorticity, concentration and temperature are stored on another set of nodes. The discretized equations are derived using the central differences for spatial derivatives and backward differences for time derivatives. A line-by-line tridiagonal matrix algorithm with relaxation is used in conjunction with iteration to solve the nonlinear discretized equations. We consider that convergence is reached when

$$\frac{|f_{i,j}^{m+1} - f_{i,j}^{m}|}{\max|f_{i,j}^{m}|} \leqslant \varepsilon \tag{16}$$

where f corresponds to the variables (ω, ψ, n, T) and ε is the prescribed tolerance, m is the iteration number, and i,j denote the grid points. To check the grid independence of the solutions, grid size was varied from 21×21 to 81×81. The result of this study is presented in Table 1. We can see that the variation in the last two cases is less than 3.5×10^{-4}, which is negligibly small. Hence, the results presented here are obtained for a square enclosure with 61×61 grid size ($\Delta x = \Delta y = 0.016$), $\Delta t = 0.001$ and $\varepsilon = 10^{-6}$.

The code was validated with the case of double diffusion for the case $A = 1.5$, $Ra_T = 40\,000$, $Ra_s = -10^5$, $Pr = 1$, $Le = 10^{1/2}$ [20]. The results showed that the present code reproduced exactly the same iso-patterns of Q, T and S (not shown here). Despite the fact that the referenced study was carried out by finite element method and ours by control volume method, the quantitative comparison presented in Table 2 shows very good agreement for ψ_{max}, ψ_{min}, as well as for Nusselt and Sherwood numbers, Nu_m and

Table 1
Grid independence study with $Ra_T = 0$, $Sc = 1$, $Pe = 10$ and $Ra = 10^3$

$N_x \times N_y$	21×21	41×41	61×61	81×81
ψ_{max}	5.559	5.572	5.577	5.579
n_{max}	21.061	18.059	17.239	17.082

Table 2
Validation of the code with the case of double diffusion for the case $A = 1.5$, $Ra_T = 40{,}000$, $Ra_s = -10^5$, $Pr = 1$, $Le = 10^{1/2}$ [20]

	ψ_{max}	ψ_{min}	Nu_m	Sh_m	$N_x \times N_y$	Δt
Mamou et al. [20]	10.126	−10.126	2.546	3.741	24×20	2×10^{-4}
This code	10.090	−10.090	2.533	3.726	61×41	1×10^{-3}
(%) Variation	0.36	0.36	0.51	0.40		

Sh_m. As a further test, we run the code to simulate the Bénard problem [21] and found excellent agreement, which we will present later.

4. Results and discussion

Computations are performed for the following values of dimensionless parameters: $Sc = 1$, $Le = 1$, $Pe = 10$, which correspond to typical bioconvection cases with known microorganism characteristics (e.g. [22]) and Ra_T and Ra are variable. Fig. 2 displays the bifurcation diagram (ψ_{max} vs. Ra_T) for the case of no bioconvection, $Ra = 0$. A bifurcation between purely conductive and convective states is clearly seen at around the Rayleigh number of 1708, which is the critical Rayleigh number of a horizontal fluid layer heated from below by a constant temperature. This situation corresponds to the classical Bénard problem, mentioned earlier [21].

Fig. 3 shows the bifurcation curve (ψ_{max} vs. Ra) for the case of isothermal cavity ($Ra_T = 0$). This figure is obtained by beginning the simulation with the diffusion state (i.e. no convection) as initial condition, gradually increasing the Rayleigh number until convection arises, and continuing to obtain solutions at higher Rayleigh numbers with the solution at the previous (lower) Rayleigh number as initial condition. Once the solution at the highest Rayleigh number is obtained, we proceed backward to obtain solutions at lower Rayleigh numbers using the solution at the previous (higher) Rayleigh number as initial condition. Similar to the case of a vertical cylinder [23], it is found that the bioconvection arises (as the Rayleigh number Ra is increased) at a certain *supercritical* value, $Ra_c^{sup} = 1100$ and disappears suddenly (as Ra is decreased) at a certain *subcritical* value, Ra_c^{sub} with $Ra_c^{sub} < Ra_c^{sup}$. This behaviour is typical of a subcritical bifurcation. It has also been observed experimentally by Mogami et al. [24] which analysed the temporal and spatial changes in bioconvection pattern with varying gravity. They found a lower threshold, i.e. a lower critical Rayleigh number, for decreasing gravity than for increasing gravity.

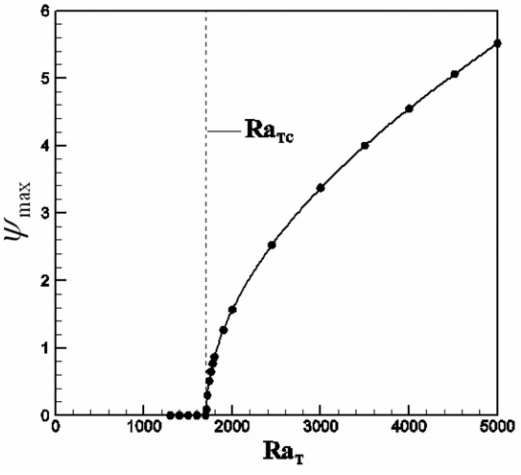

Fig. 2. Bifurcation diagram for $Ra = 0$ (no bioconvection).

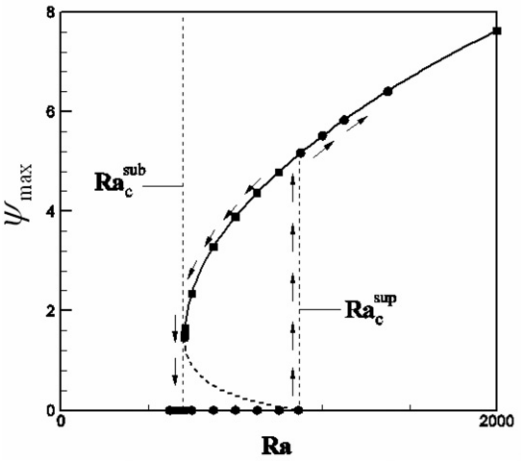

Fig. 3. Bifurcation diagram for $Ra_T = 0$ (no thermal effect).

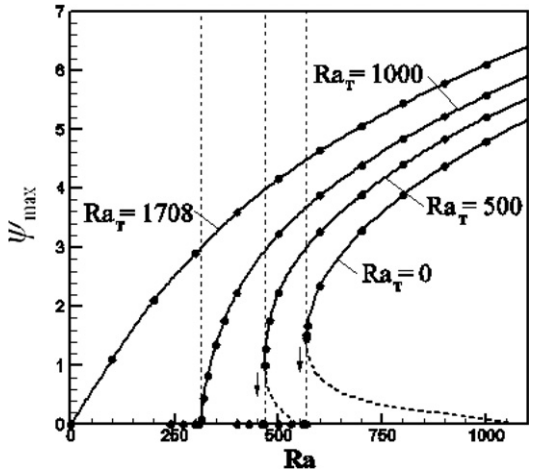

Fig. 4. Bifurcation diagram for $Ra_T = 0, 500, 1000$ and 1708.

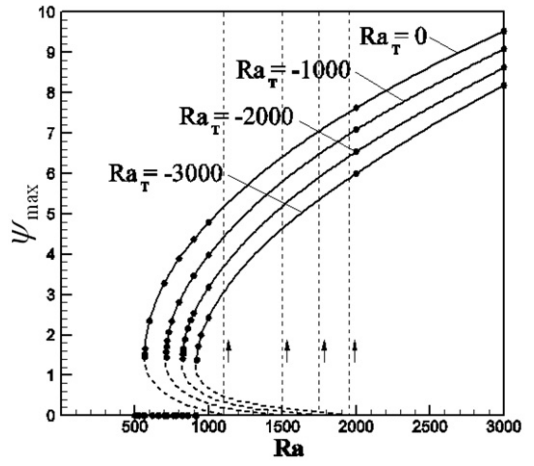

Fig. 5. Bifurcation diagram for $Ra_T = 0$, -1000, -2000 and -3000.

The effect of heating from below on the form of bifurcation diagram is presented in Fig. 4 for four fixed values of Ra_T of 0, 500, 1000 and 1708. The thermal Rayleigh number Ra_T characterizes the temperature difference between the horizontal walls of the cavity. Thus, as can be observed from Fig. 4, the onset of convection is strongly subcritical when $Ra_T = 0\,(Ra_c^{sub} = 1100)$, however we report a transition from subcritical bifurcation to supercritical bifurcation when the thermal Rayleigh number is increased from 0 to 1708: at $Ra_T = 500$, it is still subcritical, $Ra_c^{sub} = 550$, it becomes supercritical $Ra_c^{sup} = 320$ at $Ra_T = 1000$ and finally it is $Ra_c^{sup} = 0$ at $Ra_T = 1708$.

The bifurcation diagrams for the case of cooling from below is presented in Fig. 5 for the values of thermal Rayleigh number of $0, -1000, -2000$ and -3000. The results indicate that the bifurcation remains subcritical when the thermal Rayleigh number is decreased from 0 to -3000: it is $Ra_c^{sub} = 1100$ at $Ra_T = 0$, it is $Ra_c^{sup} = 1490$ at $Ra_T = -1000$, it is $Ra_c^{sup} = 1760$ at $Ra_T = -2000$ and finally it is $Ra_c^{sup} = 1980$ at $Ra_T = -3000$.

To examine the flow, concentration and temperature patterns during transition from subcritical to supercritical, the streamlines, isoconcentration and isotherms for Ra_T of 0, 500 and 1000 of Fig. 4 are plotted in Fig. 6. We see that for $Ra_T = 0$, the subcritical Rayleigh number is $Ra_c^{sub} = 567$ with $\psi_{max} = 1.46$. The convective cell is asymmetric and shifted to the right corner, and following the same pattern, the cells are concentrated to the right corner. The isotherms show quasi-convection regime following the same trend of the streamlines. For $Ra_T = 500$, the subcritical Rayleigh number is slightly decreased to $Ra_c^{sub} = 468$ with a reduced strength of circulation of $\psi_{max} = 0.99$. We can see however that the basic pattern did not change in all three isolines for $Ra_T = 0$ and 500. For $Ra_T = 1000$, the critical Rayleigh number is $Ra_c^{sub} = 315$ and the strength of circulation is reduced considerably to $\psi_{max} = 0.08$. The convective cell is symmetric, so is the cell concentration at the top boundary and the isotherms show a conduction dominated regime. Thus, it is clearly seen that for $Ra_T = 0$ and 500 the conduction regime is not reached showing the presence of a supercritical state. In contrast, for $Ra_T = 1000$, the conduction regime is reached at subcritical state.

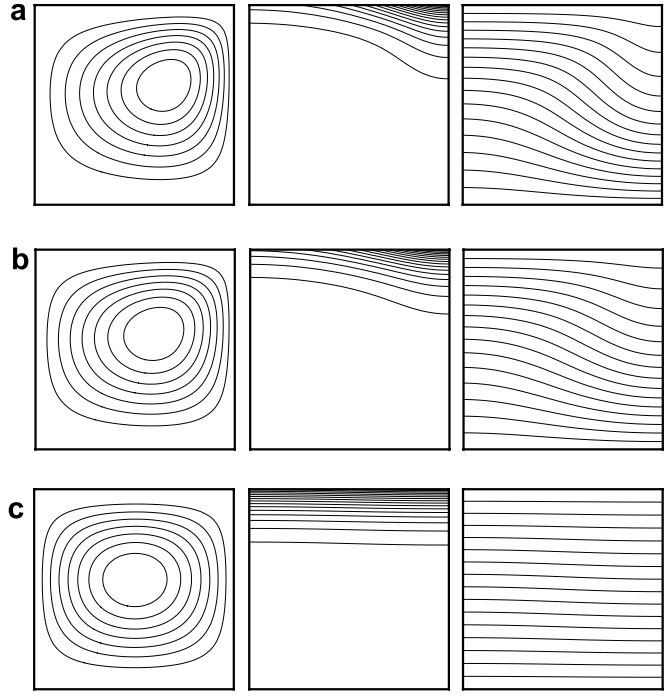

Fig. 6. Streamlines, isoconcentration and isotherm for $Ra_T = 0, 500$ and 1000 at their subcritical Ra_c^{sub} of Fig. 4. (a) $Ra_{T=}0$, $Ra_c^{sub} = 567$, $\psi_{max} = 1.46$, (b) $Ra_T = 500$, $Ra_c^{sub} = 468$, $\psi_{max} = 0.99$, (c) $Ra_T = 1000$, $Ra_c^{sub} = 315$, $\psi_{max} = 0.08$.

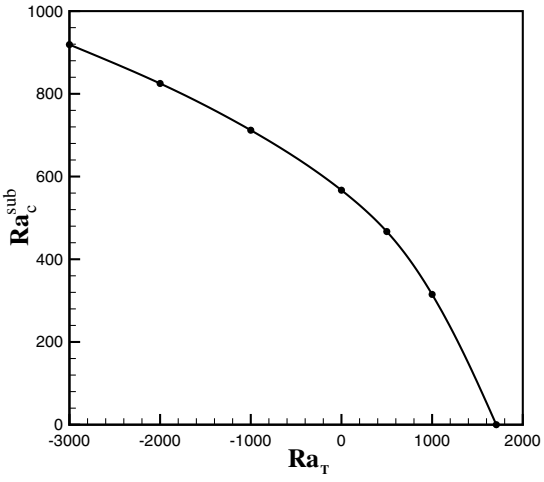

Fig. 7. Effect of thermal Rayleigh number on subcritical bioconvection Rayleigh number.

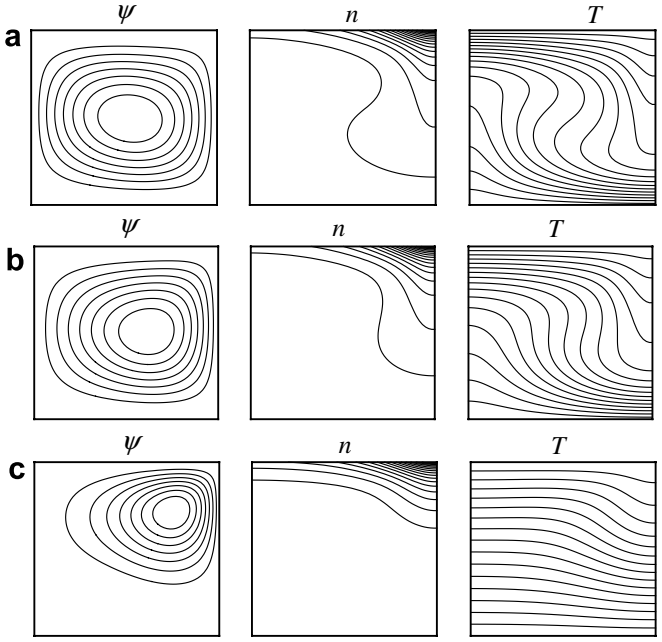

Fig. 8. Streamlines, isoconcentration and isotherm for $Ra = 10^3$: (a) $Ra_T = 4 \times 10^3$, $\psi_{max} = 7.63$, (b) $Ra_T = 0$, $\psi_{max} = 4.97$, (c) $Ra_T = -4 \times 10^3$, $\psi_{max} = 1.35$.

The subcritical Rayleigh number, Ra_c^{sub} of Figs. 4 and 5 as a function of the thermal Rayleigh number, Ra_T is presented in Fig. 7. It is clear that the subcritical bioconvection Rayleigh number decreases with the thermal Rayleigh number. This means that increasing the temperature gradient between top and bottom of the enclosure destabilizes the suspension and helps to develop the bioconvection.

The influence of the thermal Rayleigh number, Ra_T from -4000 to $+4000$ is illustrated in Fig. 8, in terms of the streamlines (left), isoconcentration (center) and isotherms (right) for $Ra = 10^3$. Since both Rayleigh numbers are high and Ra_T corresponds to cooling as well as heating from below, we expect to see clearly the influence of Ra_T for both cases on the iso-patterns, which is indeed the case: the thermal Rayleigh number has a strong effect on the convective flow patterns. This is examined in conjunction with the horizontal profiles of ψ, n and T at the mid-height of enclosure ($y = 0.5$), shown in Fig. 9a–c, and also with the vertical profiles of ψ, n and T at the mid-width of enclosure ($x = 0.5$) shown in Fig. 9d–f. For cooling from below, we notice that the convective cell shifts to the top right of the cavity as seen in Fig. 8c, and the horizontal and vertical profiles of the stream function become asymmetrical, Fig. 9a and d. On the other hand, the heating from below tends to center the convective cell in the cavity and thus makes the profiles symmetrical. We can also note that for heating from below, the value of the stream function increases, which is to say, the convection is reinforced. For cooling from below, the stream function is decreased and the flow strength is weakened. We see in Fig. 9b and e that the gradient of concentration of microorganisms

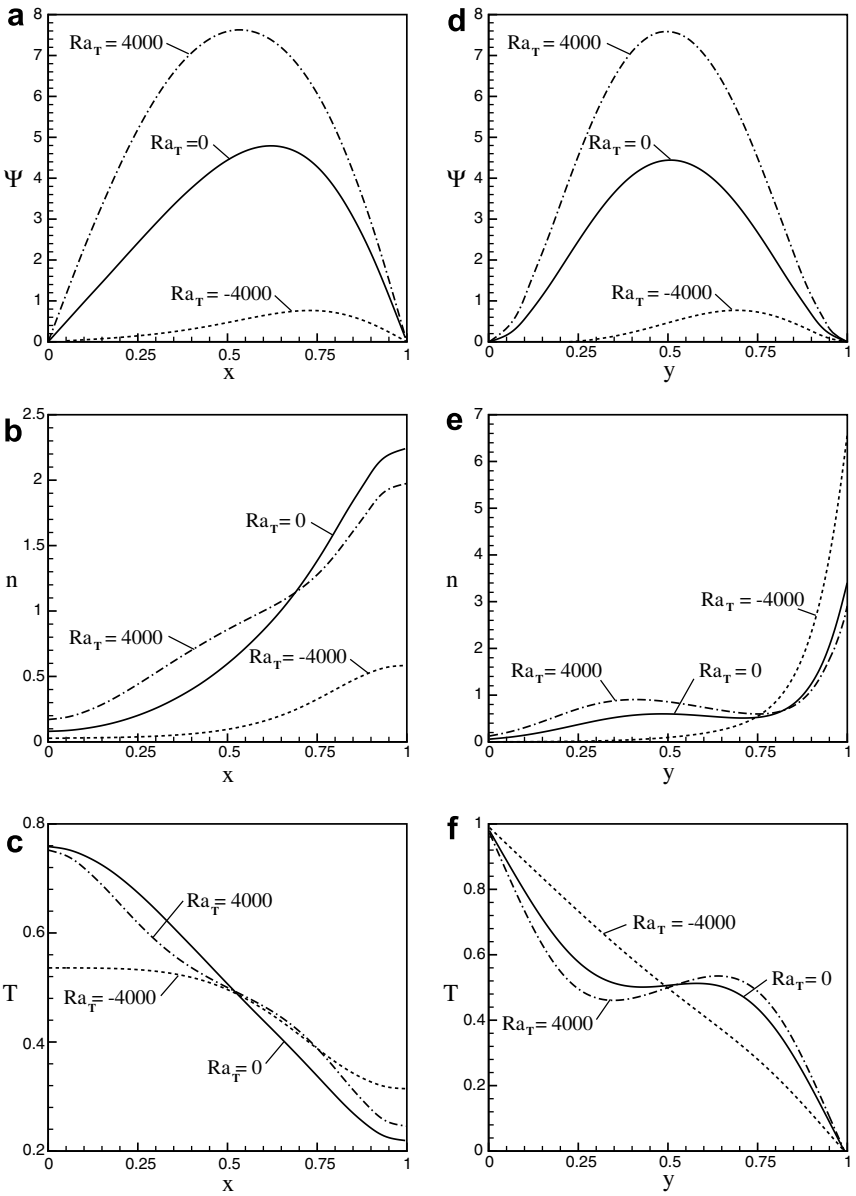

Fig. 9. Effect of thermal Rayleigh number on horizontal and vertical profiles at the mid-height ($y = 0.5$) and mid-width ($x = 0.5$) of the enclosure, respectively, for $Ra = 10^3$.

remains high at the upper boundary and its maximum is at the right corner of the cavity. For cooling from below, in Fig. 9f, the vertical temperature profile becomes almost linear and approaches the state of pure conduction. This is expected in view of the isotherms which are almost vertical lines in Fig. 8c.

5. Conclusion

Numerical simulations of thermo-bioconvection in a square enclosure were carried out. The vertical walls of the cavity are assumed to be stress-free and insulated, while horizontal boundaries are rigid. The vertical gradient of temperature is established by maintaining the horizontal boundaries at fixed temperatures. Both cases of heating or cooling from below were examined. The governing equations are integrated numerically using the control volume method. The present results exhibit the influence of thermo-effects on the bifurcation diagram and the flow structure. We have reported a transition from a subcritical bifurcation to a supercritical bifurcation when the thermal Rayleigh number is increased from 0 to 1708, while the bifurcation remains subcritical when the cooling from below is applied. Our result indicates also that the heating from below destabilizes the suspension and cooling from below stabilizes it.

Acknowledgement

The financial support for this study by Natural Sciences and Engineering Research Council Canada is acknowledged.

References

[1] N.A. Hill, T.J. Pedley, J.O. Kessler, The growth of bioconvection patterns in a suspension of gyrotactic micro-organisms in a layer of finite depth, J. Fluid Mech. 208 (1989) 509–543.
[2] A.J. Hillesdon, T.J. Pedley, Bioconvection in suspensions of oxytactic bacteria: linear theory, J. Fluid Mech. 324 (1996) 223–259.
[3] A.M. Metcalfe, T.J. Pedley, Falling plumes in bacterial bioconvection, J. Fluid Mech. 445 (2001) 121–149.
[4] T.J. Pedley, J.O. Kessler, Hydrodynamic phenomena in suspensions of swimming microorganisms, Ann. Rev. Fluid Mech. 24 (1992) 313–358.
[5] N.A. Hill, T.J. Pedley, Bioconvection, Fluid Dyn. Res. 37 (2005) 1–20.
[6] S. Childress, M. Levandowsky, E.A. Spiegel, Pattern formation in a suspension of swimming microorganisms: equations and stability theory, J. Fluid Mech. 63 (1975) 591–613.
[7] S. Fujita, M. Watanabe, Transition from periodic to non-periodic oscillation observed in a mathematical model of bioconvection by motile micro-organisms, Physica D: Nonlinear Phenomena 20 (1986) 435–443.
[8] A. Harashima, M. Watanabe, L. Fujishiro, Evolution of bioconvection patterns in a culture of motile flagellates, Phys. Fluids 31 (1988) 764–775.
[9] S. Ghorai, N.A. Hill, Development and stability of gyrotactic plumes in bioconvection, J. Fluid Mech. 400 (1999) 1–31.
[10] S. Ghorai, N.A. Hill, Wavelengths of gyrotactic plumes in bioconvection, Bull. Math. Biol. 62 (2000) 429–450.
[11] S. Ghorai, N.A. Hill, Periodic arrays of gyrotactic plumes in bioconvection, Phys. Fluids 12 (2000) 5–22.
[12] S. Ghorai, N.A. Hill, Axisymmetric bioconvection in a cylinder, J. Theor. Biol. 219 (2002) 137–152.
[13] T.J. Pedley, N.A. Hill, J.O. Kessler, The growth of bioconvection patterns in a uniform suspension of gyrotactic micro-organisms, J. Fluid Mech. 195 (1988) 223–237.
[14] A.V. Kuznetsov, The onset of bioconvection in a suspension of gyrotactic microorganisms in a fluid layer of finite depth heated from below, Int. Commun. Heat Mass Transfer 32 (2005) 574–582.
[15] A.V. Kuznetsov, Thermo-bioconvection in a suspension of oxytactic bacteria, Int. Commun. Heat Mass Transfer 32 (2005) 991–999.
[16] A.V. Kuznetsov, Investigation of the onset of thermo-bioconvection in a suspension of oxytactic microorganisms in a shallow fluid layer heated from below, Theor. Comput. Fluid Dyn. 19 (2005) 287–299.
[17] D.A. Nield, A.V. Kuznetsov, The onset of bio-thermal convection in a suspension of gyrotactic microorganisms in a fluid layer: oscillatory convection, Int. J. Therm. Sci. 45 (2006) 990–997.
[18] Z. Alloui, T.H. Nguyen, E. Bilgen, Stability analysis of thermo-bioconvection in suspensions of gravitactic micro-organisms in a fluid layer, Int. Commun. Heat Mass Transfer, doi:10.1016/j.icheatmasstransfer.2006.08.012.
[19] S.V. Patankar, Numerical Heat Transfer and Fluid Flow, McGraw Hill, New York, 1980.
[20] M. Mamou, P. Vasseur, M. Hasnaoui, On numerical stability analysis of double-diffusive convection in confined enclosures, J. Fluid Mech. 433 (2001) 209–250.
[21] A. Pellew, R.V. Southwell, On maintaining convective motion in a fluid heated from below, Proc. R. Soc. Series A, Math. Phys. Sci. 176 (1940) 312–343.
[22] T. Kawakubo, Y. Tsuchiya, Diffusion coefficient of paramecium as a function of temperature, J. Protozool 28 (3) (1981) 342–344.
[23] Z. Alloui, T.H. Nguyen, E. Bilgen, Bioconvection of gravitactic microorganisms in vertical cylinder, Int. Commun. Heat Mass Transfer 32 (2005) 739–747.
[24] Y. Mogami, A. Yamane, A. Gino, S.A. Baba, Bioconvective pattern formation of *Tetrahymena* under altered gravity, J. Exp. Biol. 207 (2004) 3349.